Indoor Air 1999; 9: 125–133
Printed in Denmark. All rights reserved

ISSN .

AIVC 12,383

Room Airflow Studies Using Sonic Anemometry

PIOTR T. WASIOLEK*, JEFFREY J. WHICKER, HONGRUI GONG AND JOHN C. RODGERS

Abstract To ensure prompt response by real-time air monitors to an accidental release of toxic aerosols in a workplace, safety professionals should understand airflow patterns. This understanding can be achieved with validated computational fluid dynamics (CFD) computer simulations, or with experimental techniques, such as measurements with smoke, neutrally buoyant markers, trace gases, or trace aerosol particles. As a supplementary technique to quantify airflows, the use of a state-of-the art, three-dimensional sonic anemometer was explored. This instrument allows for the precise measurements of the air-velocity vector components in the range of a few centimeters per second, which is common in many indoor work environments. Measurements of air velocities and directions at selected locations were made for the purpose of providing data for characterizing fundamental aspects of indoor air movement in two ventilated rooms and for comparison to CFD model predictions. One room was a mockup of a plutonium workroom, and the other was an actual functioning plutonium workroom. In the mockup room, air-velocity vector components were measured at 19 locations at three heights (60, 120 and 180 cm) with average velocities varying from 1.4 cm s^{-1} to 9.7 cm s^{-1}. There were complex flow patterns observed with turbulence intensities from 39% up to 108%. In the plutonium workroom, measurements were made at the breathing-zone height, recording average velocities ranging from 9.9 cm s^{-1} to 35.5 cm s^{-1} with turbulence intensities from 33% to 108%.

Key words Sonic anemometer; Indoor air velocity; Indoor turbulence; Airflow patterns.

Received 21 August 1998. Accepted for publication 29 December 1998

Introduction

The need for airflow measurements in a work place has been recognized by health and safety professionals not only as a problem of workplace comfort, but also as a potential tool in designing engineering measures to reduce accidental exposures of workers to toxic aerosols. A specific case is the radiation protection of workers in nuclear facilities. The possibility of accidental airborne releases of radionuclides during the handling and processing of radioactive materials, which are not detectable by human senses, is a fact of which every health physicist is constantly aware. The proper placement of alarming devices in a nuclear workplace, such as continuous air monitors (CAMs), is a factor in determining how effectively these devices respond to accidental release of radioactive gases and aerosols (Crites, 1994). Accordingly, an understanding of airflow patterns and their effect on dispersal of the radioactive material in the room can be an effective tool in improving CAM performance.

Another reason for determining the airflow patterns is to help in design of workplace ventilation systems, including the placement and shape of inlet and outlet registers to remove accidentally released airborne radioactivity from the workers' breathing zone as quickly as possible and thus minimize harmful exposure. Several qualitative tracing techniques such as neutral buoyancy balloons, smoke, trace gases, and trace particles have been tried in the past with mixed results (Vavasseur et al., 1986; Mishima et al., 1988; Whicker et al., 1997). The main disadvantages of these techniques are the qualitative nature of the results, or difficulties in performing actual measurements. Quantitative techniques, such as thermal anemometry and Laser Doppler Velocimetry (LDV), have also been used to measure indoor airflows. These techniques have provided valuable information regarding room airflows, but also have limitations. For example, the velocity threshold of hot-wire systems is around 10–15 cm s^{-1}, without special calibrations, which is too large for typically encountered indoor air velocities (Matthews et al., 1989; Papadopoulos et al., 1996). The LDV technique described in Polyakov (1988) has the potential of being a valuable tool for air velocity measurements in wide range of velocities and sampling frequencies, but the need for release of seed particles and the high cost of current LDV systems limits its application.

An alternative non-instrumental method that can be used for airflow pattern predictions is numerical simu-

*Health Physics Measurements Group, ESH-4, Los Alamos National Laboratory, MS G761, Los Alamos, NM 87545, USA, Tel: +1 505 667 0198, Fax: +1 505 665 6071, e-mail: wasiolek@lanl.gov, *Author to whom correspondence should be addressed*

lation via computational fluid dynamics (CFD) computer models of room geometry and flow boundary conditions, coupled with physical models of particle response to the predicted flow field (Hirt et al., 1979; Kurabuchi et al., 1990; Awbi, 1991; Skovgaard and Nielsen, 1991; Buchanan, 1997). However, experimental validation of such CFD computer models has remained a serious limitation in applying them with a high degree of confidence to workplaces that have complex configurations.

An experimental technique that may contribute to airflow studies and help in validation of the CFD models is direct measurement of three-dimensional flow fields using state-of-the art sonic anemometry. This technique provides highly accurate three-dimensional measurements of the air-velocity vector components in the range of centimeters per second. Two earlier attempts in using sonic anemometers for indoor airflow studies (Irwin and Paumier, 1990; Yost and Spear, 1992) were only partially successful and were limited by the lack of sensitivity to low air velocities of the older instruments. Sonic anemometers used in these two previous studies had a threshold of velocity in the range of 2 to 5 cm s^{-1}, implying that up to 20% of measured velocity components were below the instruments' detection limits. Recent technological improvements in ultrasound technology, combined with transducers that are more accurate and faster, have resulted in more accurate and sensitive commercial sonic anemometers. Current instruments from different manufacturers have the ability to detect air velocities in a millimeter per second range, although in some cases, a special calibration may be required. The results of the application of the sonic anemometry in support of the radiation protection program at Los Alamos National Laboratory (LANL) are presented here.

The primary goal of this project was to use sonic anemometry to measure the airflow quantities of velocity and turbulence in a mockup room for comparison with measurements in the active plutonium workroom. These measurements could then be used to increase our understanding of the fundamental mechanisms involved in dispersion of toxic materials into a workroom. In addition, this data set can be used to validate CFD model prediction. Ultimately, this information could be used to increase worker protection from other inhalation hazards.

Material and Methods

Experimental Room

The obvious technical difficulties of making extensive airflow measurements in a production facility handling nuclear materials forced the construction of an experimental mockup room simulating a real workroom. The mockup room used in this study is a freestanding structure located within a larger building. The room is a modular metal-wall structure with dimensions of 6.1×4.8×2.4 m (V=70.3 m^3) and is furnished with mockup gloveboxes and an overhead passbox (a sealed tunnel used for moving radioactive samples between gloveboxes in a plutonium facility) inside. A schematic diagram of the room is presented in Figure 1. The room is supplied with close-looped high-efficiency particulate filter (HEPA)-filtered air through four 0.2-m diameter inlet registers in the ceiling equipped with 0.3-m diameter horizontal deflecting plates. Four 0.2-m diameter adjustable exhaust registers are located in the room corners, 0.3 m above the floor. The nominal air exchange rate was set to 6 h^{-1}. Measurements of the volumetric flow rate at the inlet and outlet registers using an industrial flow measurement instrument (Model CFM-88-1, Shortridge Instruments, Scottsdale, AZ, USA) yielded average values presented in Table 1. The near-uniform distribution of air velocities around the deflector plates was verified by measurements with a hot wire anemometer (Model 630, Sierra Instruments, Carmel Valley, CA, USA) at the edge of the deflector plates. As the experimental room is located indoors with a thermally insulated floor, there was no significant (less than 0.5°C) temperature gradient detected between opposite walls (including ceiling and floor), as measured with fine wire thermocouples (Model FW05, Campbell Scientific, Inc., Logan, UT, USA).

The 19 locations marked in Figure 1 were selected for measurements of air velocity vectors. As the experimental room has a ceiling-mounted passbox, the sampling heights varied depending on location. At locations 7, 8, 9, the two sampling heights were 60 and 120 cm, whereas for all others the sampling heights were 60, 120 and 180 cm above the room floor. Sonic anemometer was positioned 50 cm from glovebox faces and the room walls. Experimental room measurements were performed under steady-state conditions, established by waiting for at least 10 min (one nominal air exchange) after closing and sealing the room door. The remaining room openings (e.g., sampling or cable

Table 1 Volumetric flow rate at inlet and outlet registers

Location	Inlet ($\times 10^{-3}$ $m^3 s^{-1}$)	Outlet ($\times 10^{-3}$ $m^3 s^{-1}$)
SW	38.9	33.6
SE	33.8	35.9
NE	27.6	31.4
NW	32.0	33.0
Total	132.3	133.9

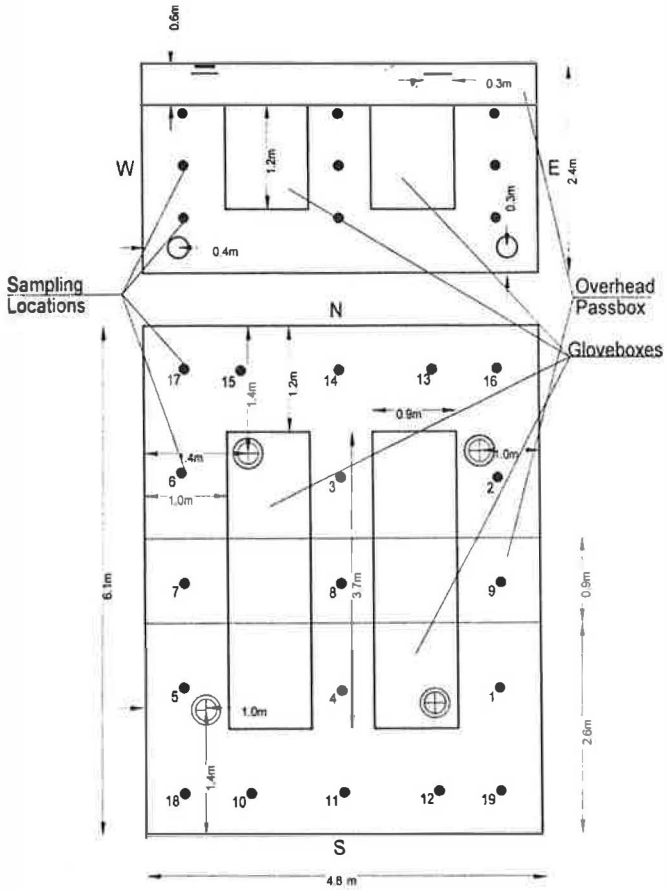

Fig. 1 Schematic diagram with sampling locations of the experimental mockup facility

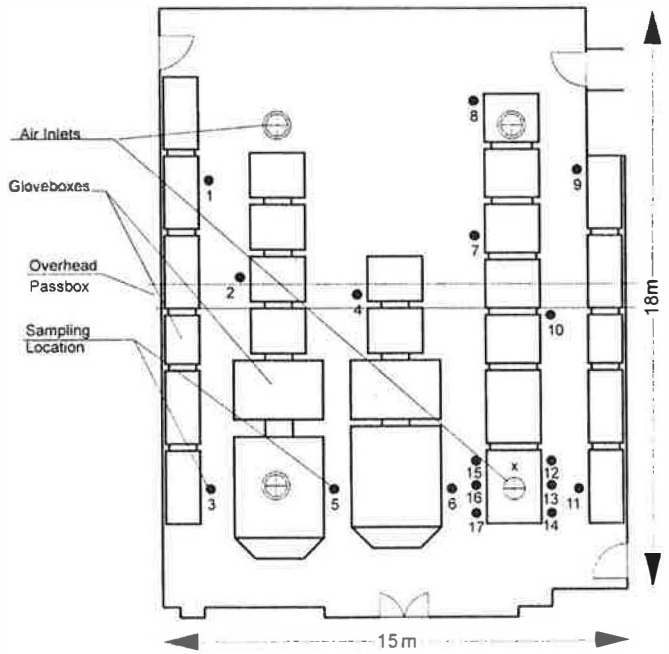

Fig. 2 Schematic diagram with sampling locations of a plutonium workroom at LANL

ports) were sealed, although it was not intended to make the room completely air tight.

Plutonium Facility

The schematic diagram of a workroom in the LANL plutonium-handling facility, accessible for the airflow study, is presented in Figure 2. The room dimensions are 15×18×5 m. Several rows of gloveboxes and an overhead transport passbox were present in the room. HEPA-filtered air is supplied into the room through four ceiling registers. The four rectangular outlet registers (0.3×0.6 m) are located in the room corners 0.3 m above floor. The nominal air exchange rate was 10 h^{-1}. Because this is a plutonium handling facility with restricted access, only a limited number of sampling locations (marked in Figure 2) were available for this study. A sampling location at a height of 150 cm and 30 cm from the glovebox face was selected to represent the breathing zone of a worker. All measurements were performed with people present in the room; however, an attempt was made to have no one in the vicinity of the sonic anemometer sampling head.

Sonic Anemometry

To characterize the airflow patterns we used a commercial sonic anemometer (Model CSAT3, Campbell Scientific, Inc., Logan, UT, USA). The critical dimensions of its sampling head geometry are presented in Figure 3. The sonic anemometer measures the time of flight of pulsed sound waves across a 10-cm measurement path. From these measurements the three orthogonal air velocity components are determined with a programmable sampling rate that can be set from 1 to 60 Hz. To measure air velocity on each axis, two ultrasonic signals are pulsed in opposite directions. The times of flight of the first signal (out), t_{out}, and second signal (back) t_{back}, are given by,

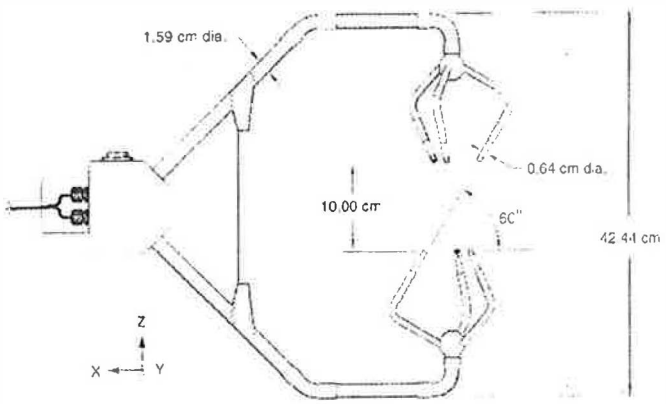

Fig. 3 Geometry of sonic anemometer sampling head (courtesy of Campbell Scientific, Inc)

$$t_{out} = \frac{d}{c+u_a} \quad (1)$$

$$t_{back} = \frac{d}{c-u_a} \quad (2)$$

where u_a is the first nonorthogonal wind component along the transducer axis, d is the distance between transducers, and c is the speed of sound. From the above equations, the wind speed along any axis can be found by solving for u_a:

$$u_a = \frac{d}{2}\left[\frac{1}{t_{out}} - \frac{1}{t_{back}}\right] \quad (3)$$

All of the nonorthogonal wind speed components are then transformed into orthogonal wind speed components u_x, u_y and u_z that are referenced to the axes of anemometer head with a 3×3 transformation matrix, A:

$$\begin{bmatrix} u_x \\ u_x \\ u_z \end{bmatrix} = A \begin{bmatrix} u_a \\ u_b \\ u_c \end{bmatrix} \quad (4)$$

As the expected air velocities were small, a special custom calibration and instrument adjustments were performed in the manufacturer's wind tunnel facility.

The results of this new, custom calibration for all three velocity-vector components yielded average threshold velocity values of 0.2 cm s^{-1} at 21°C. These values are an order-of-magnitude smaller than the standard factory calibration and far below the guaranteed value of 4 cm s^{-1} that is derived for a much wider temperature range outdoors. The accuracy of several sonic anemometers, including a model (CSAT3) similar to the one used in this project, was evaluated by Vogt (1997). According to his wind tunnel studies, the average difference between CSAT3 and the reference wind speed values was −1.1%. The minimum and maximum difference between the measured wind speed and the reference tunnel speed for all tested wind speeds and angle of attack were −10.3% and +6.0%, respectively.

The sonic anemometer head was mounted on a mobile cart for ease of transport and leveled after any change in sampling location. The mounting arrangement allowed for changes in the sampling height. The sonic anemometer head (Vogt, 1997) and the mobile cart were designed to minimize local airflow disturbance.

In the mockup room every sample consisted of 600 individual measurements, as the sonic anemometer controls were set to collect data for 10 min with the sampling frequency of 1 Hz. In a plutonium workroom, due to restriction in available access time, samples consisted of only 300 measurements (5 min run). The raw, binary data files containing air velocity individual components were converted to ASCII text format, corrected for offset, and rotated to align orientation of the sonic sampling head with common room coordinates.

By vector summation of individual air velocity vector components u_x, u_y and u_z, the absolute air velocity was calculated for every sample, i, with the equation,

$$u_i\ (\text{cm s}^{-1}) = \sqrt{u_{ix}^2 + u_{iy}^2 + u_{iz}^2} \quad (5)$$

The time average velocity for a 10-min run was calculated as $\bar{u} = \frac{1}{N}\sum_{i=1}^{N} u_i$. Statistical measure of the dispersion of data of a variable A about the mean $\bar{A}$ is the unbiased variance σ_A^2 defined as,

$$\sigma_A^2 = \frac{1}{N-1}\sum_{i=0}^{i=N-1} (A_i - \bar{A})^2 \quad (6)$$

However, any turbulent variable A, can be split into mean and turbulent part as $A = \bar{A} + a'$, and the substitution of a turbulent part $a' = A - \bar{A}$ into the definition of variance gives (Stull, 1988),

$$\sigma_A^2 = \frac{1}{N-1}\sum_{i=0}^{i=N-1} (a'_i)^2 = \overline{a'^2} \quad (7)$$

Therefore, since the standard deviation is interpreted as a measure of the magnitude of the spread or dispersion of the original data from its mean, it can be used as a measure of the intensity of turbulence. The intensity of turbulence might be expected to depend on the mean wind speed, so the dimensionless measure of the turbulence intensity, K, is often normalized to the air velocity. Using average air velocity and sample standard deviations of individual air velocity vector components s_x, s_y, and s_z, the normalized turbulence intensity, K, was expressed by Yost and Spear (1992) as,

$$K\ (\%) = 100\frac{\sqrt{s_x^2 + s_y^2 + s_z^2}}{\bar{u}}. \quad (8)$$

In some publications, the turbulence intensity is defined differently (Pruppacher et al., 1982, Stull 1988).

However, to allow for comparison of results, the definition used by Yost and Spear (1992) was applied in this work.

To find the dominant frequencies of the indoor turbulence, a fast Fourier transform (FFT) was performed on selected time series data with the commercial statistical software packet STATISTICA (StatSoft, Inc., Tulsa, OK, USA). Data used for the FFT analysis were tapered at 10%, detrended, the mean value subtracted, padded to the nearest power of two, and smoothed using a five-point Hamming window, as recommended by the FFT procedure.

Results and Discussion

Flow Field

Typical results from the mockup room, in the form of projections of the appropriate air-velocity vector components on different room planes: the vertical Y-Z components projected on the central plane at x=240 cm, and the horizontal X-Y-component at z=120 cm, are presented in Figure 4.

The absolute air velocity values, as calculated with Equation 5, varied from 1.4 cm s^{-1} at location 14 (z=60 cm) to 9.7 cm s^{-1} at location 5 (z=180 cm), with an average for all locations of 3.8±1.9 cm s^{-1}. As expected, the highest velocities were registered at locations close to inlet and exhaust registers. There was a factor-two difference between average air velocities at z=60 cm and z=180 cm of 2.5 cm s^{-1} and 5.1 cm s^{-1}, respectively. Despite approximate geometrical symmetry in the design of the mockup room and similar inlet/outlet flow rates, the results showed some asymmetry.

However, even the obtained results show the complexity of the airflow pattern. In this regard, our results substantially differ from the simple uniform pattern obtained by Yost and Spear (1992) of the nearly parallel velocity vectors in their box-type test facility, and it confirms a substantial influence of objects in the room on the airflow. In addition, the results show that the complex structure of the flow field is such that the sampling density of the point measurements is not sufficient to infer general room flow pattern by spatial interpolation as was done by Yost and Spear (1992). As well, the spatial averaging required by sonic anemometer geometry has to be taken into account for comparison to CFD model predictions.

For the workroom, the X-Y velocity distribution and flow direction projection is presented in Figure 5. Despite a limited number of workroom samples, it still can be seen that the air velocities were higher than measured in the mockup room, as was expected due

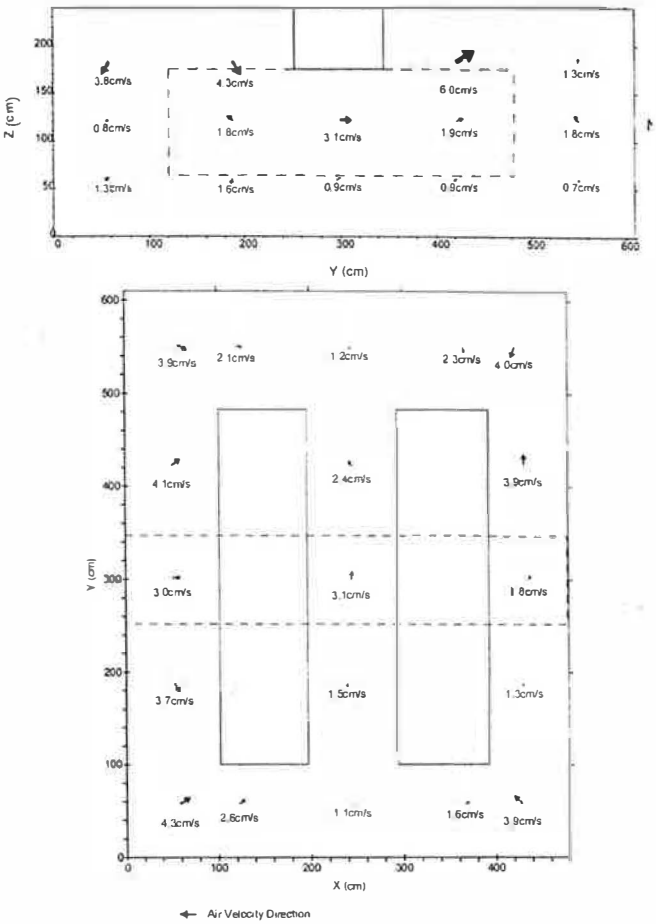

Fig. 4 Vertical and horizontal air velocity components measured at vertical (x=240 cm) and horizontal (z=120 cm) cross-sections in mockup facility

to the higher ventilation rates in the workroom. The overall average of 20.0±7.4 cm s^{-1} was nearly five times higher than the average for the mockup room. The maximum velocity of 35.5 cm s^{-1} at location 6 was nearly four times higher.

A more detailed investigation of the air velocity distribution around a glovebox (marked X in Figure 2) with six workstations equipped with circular gloveports resulted in a situation presented in Figure 6. The measurements show substantial differences in both average air velocity values (from about 20 up to 40 cm s^{-1}) and the direction of the vertical component u_z ranging from +18 cm s^{-1} (up) to −13 cm s^{-1} (down). Despite apparent symmetry of values and z-directions around two opposite sites of the glovebox, the obtained results show the difficulties in creating an effective (from the perspective of worker protection) airflow pattern that will carry contaminants away from the breathing zone. Here, for example, are two neighboring locations 13 and 14, and 16 and 17 separated by about 1 m, yet each has opposite vertical airflow

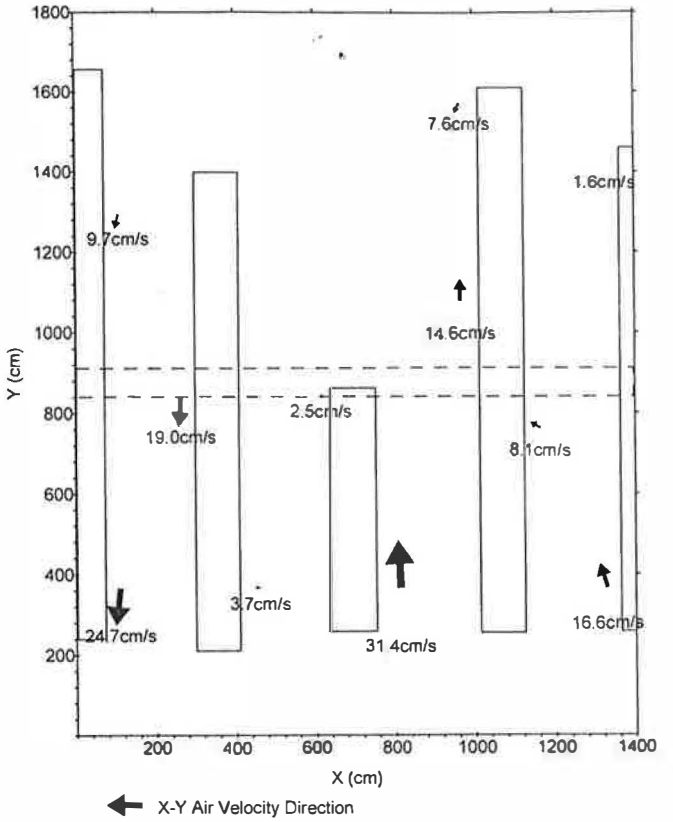

Fig. 5 Air velocity component measured at z=150 cm above the floor in a plutonium workroom

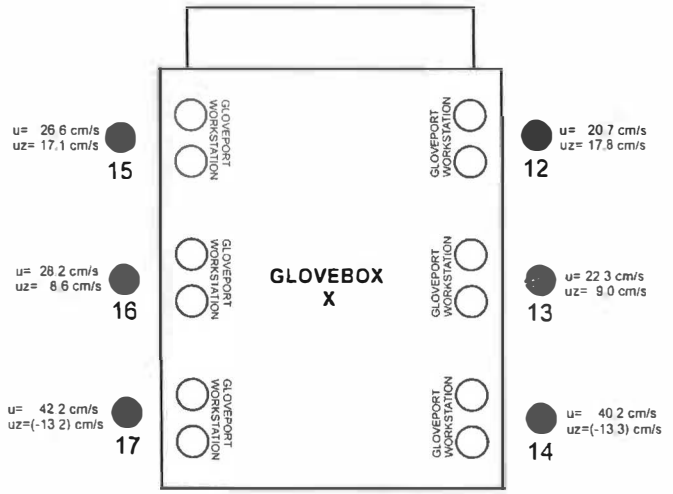

Fig. 6 Air velocity distribution around a single glovebox with six circular gloveports

directions, driving potential aerosol releases from or into the workers' breathing zone.

Turbulence Intensity

The forced ventilation, room geometry, and furnishings were expected to be possible causes of highly turbulent flow patterns both in the mockup room, as well as in the workroom. The intensity of turbulent energy transfer is an important factor in a dispersion of radioactive aerosols released accidentally, and in some cases may improve the response of real-time air monitors. On the other hand, intense turbulent energy transfer may expose other workers in the room and lead to dilution of the contaminants to such an extent there is no detector response. To quantify turbulence in a mathematical metric, the values of turbulent intensity, K, defined earlier (Equation 8) was used. The use of K is another way of analyzing the type of data that may be uniquely collected with sonic anemometry. The relative turbulence intensity based on data collected in the mockup room with the sampling frequency of 1 Hz for selected horizontal and vertical cross-sections are presented in Figurg 7. The values of K varied from 39% at location 19 (z=60 cm), to over 100% in locations 14, 15, 16 (z= 180 cm). K was high as well at some locations close to outlet registers (108% at location 10, h=60 cm). The plot of turbulence intensities in the workroom is presented in Figure 8. Comparing the workroom layout

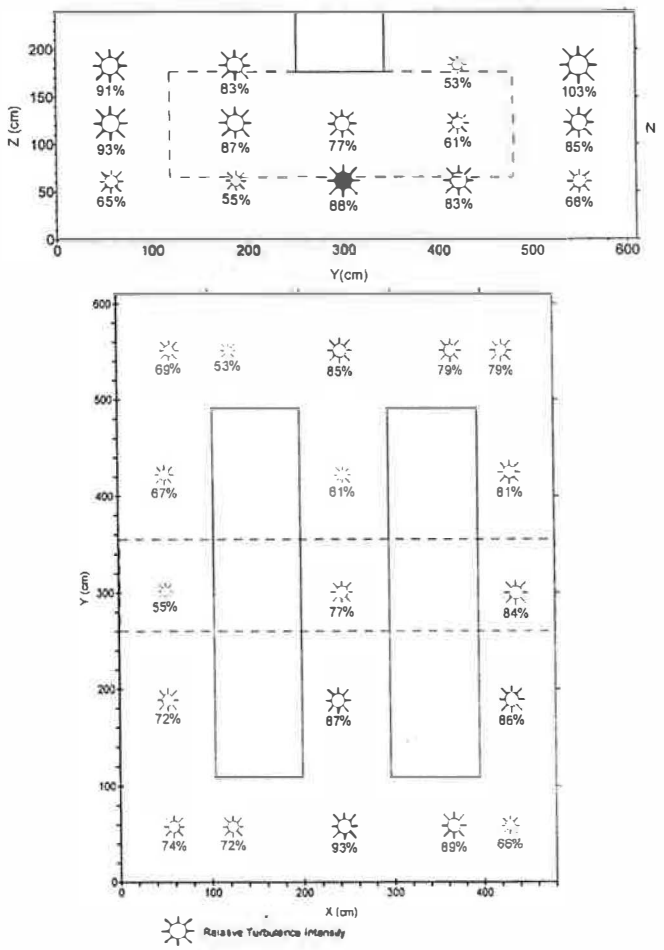

Fig. 7 Turbulence intensity calculated from measurements vertical (x=240 cm) and horizontal (z=120 cm) cross-sections in the mockup facility

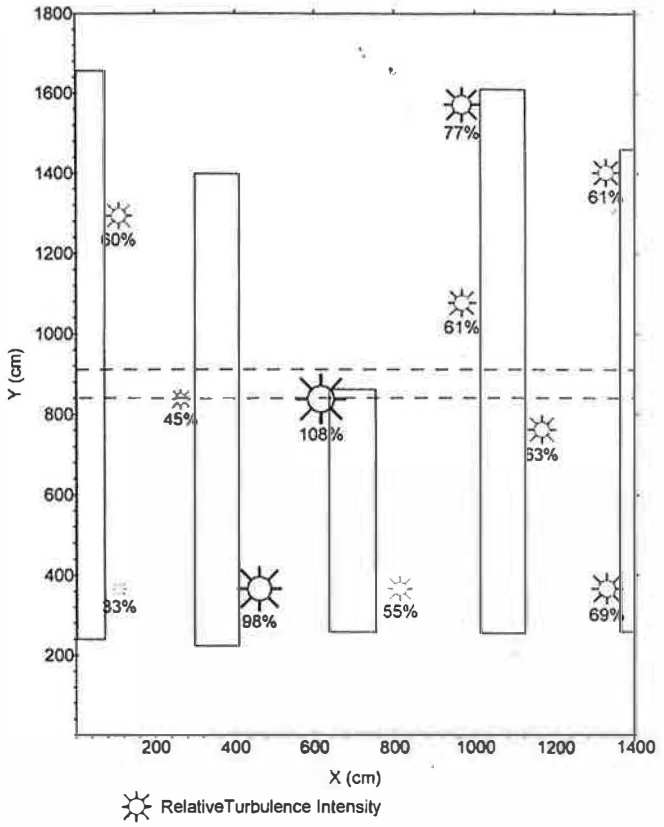

Fig. 8 Turbulence intensity distribution calculated from measurements at z=150 cm in a plutonium workroom

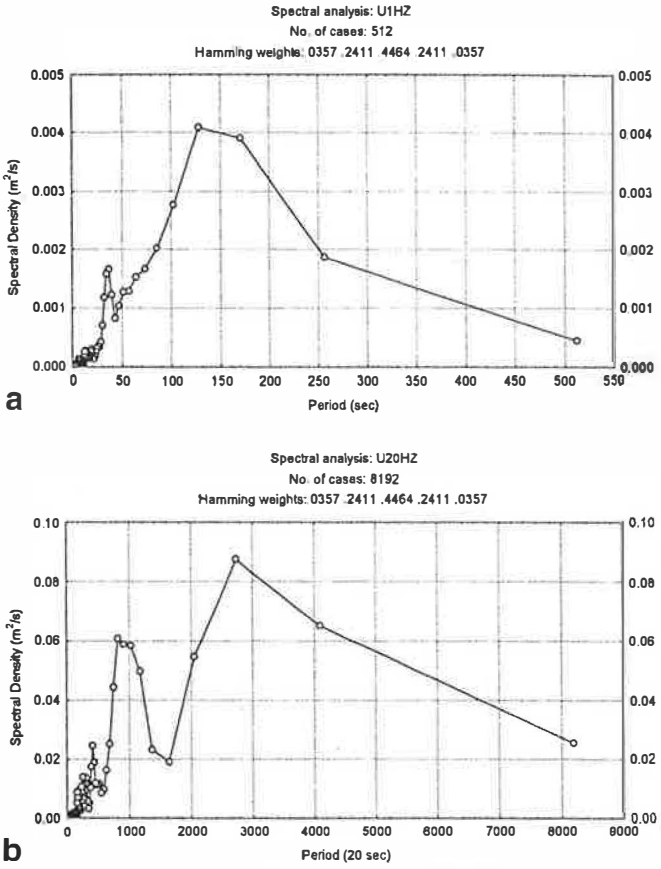

Fig. 9 Results of the fast Fourier analysis (FFT) of one data set collected in the mock-up facility (location 6) with sampling frequency of 1 Hz (a) and 20 Hz (b). Units of X-axis (period) depend on units of observation (one observation is used as the time unit, explanation in text)

(Figure 2) with the turbulence intensity plot, it can be seen, that the highest K-values of 108% and 98% were measured between gloveboxes in the center of the room (locations 4 and 5, respectively) and lower in more open spaces in the northern part of the room and along the walls. The range of measured K varied from 33% at location 3 to 108% at location 4 with an average of 64%.

As turbulence may consist of many different size eddies superimposed on each other, instrument design and the selection of sampling frequency becomes important to determined the size of the eddy that is measurable. For example, the 10-cm measurement path in the sonic anemometer used prohibits detection of smaller scale eddies. Also sampling with a frequency that is too low may also result in loss of detection of small-scale eddies.

To measure influence of varied sampling frequency on K, a set of sequential samples was collected at two locations: no. 14 (height 120 cm) in the mock-up facility and no. 6 in the plutonium workroom. Results showed no apparent changes in K with the increase of sampling frequency in the range from 1 to 60 Hz. An explanation of such behavior may be that small-scale, yet detectable with the instrument used, eddies were not present at the investigated sites. To verify such possibility, an FFT analysis was performed on the data collected in the experimental room with the sampling frequency of 1 and 20 Hz, with the results of spectral analysis presented in Figure 9a and b, respectively. Both plots show similar spectral density distributions with peaks at period values of 36 (f=0.03 Hz) and 128 s (f=0.008 Hz); and 819/20=41 s (f=0.02 Hz) and 2730/20=137 s (f=0.07 Hz), respectively. Such a two-mode distribution suggests that only a limited range of eddy frequencies, mostly in the low range (below 0.1 Hz), exist indoors and therefore increasing sampling frequency (to include higher frequency, smaller eddies) showed no effect on K. This behavior is in contrast to the outdoor environment, where small, micro-scale eddies on the order of a few millimeters in size are present – thought to be produced from the turbulent energy cascade on environmental scales (Stull, 1989).

If we assume that the eddy is frozen, (i.e., it evolves with the time scale longer than the time it takes the eddy to advect past the sensor, which is Taylor's hypothesis), the air velocity can be used to translate turbu-

lence measurements as a function of time into their corresponding measurements in space with

$$P = \frac{\lambda}{\bar{u}} \quad (9)$$

where, P is the time period, λ is the eddy diameter, and $\bar{u}$ is the mean wind velocity. Using Equation 9, results of measurements and FFT analysis, the diameters of the detected eddies can be estimated to be between about 1 m and 3 m. For comparison, a 10 cm-diameter outdoor eddy moving with wind speed of 1 m s^{-1} will result with time period of 0.1 s and frequency of 10 Hz. Additionally, with a measured velocity of 1.2 cm s^{-1} at location 14, the period of eddies smaller than the 10 cm path length of the sonic anemometer head would be less than 10 s.

Range and average values of K measured in an experimental room can be compared with values measured by Yost and Spear (1992) in their 143 m^3 experimental rectangular test chamber. Even given the 10 times higher ventilation rate of about 1 min^{-1} (60 h^{-1}) and about twice the average air velocity (9.1±4.7 cm s^{-1} in their test chamber versus 3.8±1.9 cm s^{-1} in our mockup facility), their average turbulence intensities were only 34% higher (99.3±62.2% versus 73.9±16.3%). As was the case in airflow pattern, these results confirm the strong influence of room geometry on turbulence. Computer modeling recognized that obstacles in the room influenced turbulence (Buchanan, 1997); however, no extensive experimental studies validating this have been reported.

Conclusions

Our results using sonic anemometry in the experimental room and the nuclear facility demonstrated the benefits of using advanced instrumentation for direct-air velocity measurements indoors. Moreover, the high sampling frequencies now available may provide high-resolution data on indoor turbulence. These data will prove helpful in understanding the movement and dispersion of indoor air pollutants. The sonic anemometer provides for direct measurements of air-velocity vector components and their fluctuations, which is a valuable information. This type of data will provide increase our knowledge of the fundamental aspects of indoor airflows. Also, because validation of CFD model predictions is always an issue, the availability of reliable, low-velocity flow data for direct comparison of modeling results can provide a higher level of confidence in the quality of simulated predictions. One goal of such studies is to provide tools for better understanding air movement indoors and transport of toxic aerosols, and consequently enhance the capabilities of real-time air monitors for worker protection.

Aknowledgements

The authors thank Ronald C. Scripsick and Robert A. Gore from LANL and Edward Swiatek from Campbell Scientific, Inc. for helpful discussions during preparation of this manuscript. Work supported by the U.S. DOE under Contract W7405 ENG-36.

References

Awbi, H.B. (1991) *Ventilation of Buildings*, London, E&FN Spoon.

Buchanan, C.R. (1997) "CFD characterization of mechanically ventilated office room: the effects of room design on ventilation performance", Doctoral Dissertation, Department of Mechanical and Aerospace Engineering, University of California-Irvine, Irvine, CA, USA.

Crites, T.R. (1994) "Alpha air monitor alarm sensitivity: operational experience", *Radiation Protection Dosimetry*, **53**, 65–68.

Hirt, C.W., Stein, L.R. and Scripsick, R.C. (1979) "Prediction of air flow patterns in ventilated rooms", Los Alamos, NM, Los Alamos National Laboratory Report, LA-UR-791550.

Irwin, J.S. and Paumier, J.O. (1990) "Sonic anemometer measurements within a room", Washington, DC, Environmental Protection Agency Technical Report EPA/600/D-90/036.

Kurabuchi, T., Fang, J.B. and Grot R.A. (1990) " Numerical method for calculating indoor airflows using a turbulence model", Gaithersburg, MD, National Institute of Standards and Technology Technical Report NISTIR-89/4211.

Matthews, T.G., Thompson, C.V., Wilson, D.L., Hawthorne, A.R. and Mage, D.T. (1989) "Air velocities inside domestic environments: an important parameter in the study of indoor quality and climate", *Environment International*, **15**, 545–550.

Mishima, J., Hunt, J., Kittinger, W.D., Langer, G., Ratchford, D., Ritter, P.D., Rowan, D., Stafford, R.G. and Selby, J.M. (1988) "Health physics manual of good practices for the prompt detection of airborne plutonium in the workplace", Richland, WA, Pacific Northwest Laboratory Report PNL-6612.

Papadopoulos, K.H., Soilems, A.T., Helmis, C.G., Asimakopoulos, D.N., Santamouris, W., Argiriou, A. and Dascalaki, E. (1996) "A triple hot-wire system for indoor air flow measurements", *Journal of Solar Energy Engineering*, **118**, 168–176.

Polyakov, A.F. (1989). "Thermo- and Laser Anemometry", New York, Hemisphere Publishing Corporation.

Pruppacher, H.R., Semonian, R.G. and Slinn, W.G.N. (1982) "Precipitation, scavenging, dry deposition, and resuspension", In: Proceedings of the *Fourth International Conference on Precipitation Scavenging, Dry Deposition, and Resuspension*, Santa Monica, CA, USA.

Stull, R.B. (1988) *An Introduction to Boundary Layer Meteorology*, Dordrecht, The Netherlands, Kluwer Academic Publishers.

Vavasseur, C., Muller, J.P., Asubertin, G. and Levevre, A. (1986) "Application of tracer gas methods to the measurements of ventilation parameters in nuclear power plants and various industrial sectors", In: Goodfellow, H.D. (ed.)

Ventilation '85, Amsterdam, The Netherlands, Elsevier Science Publishers B.V.

Vogt, R. (1997) "Intercomparison of ultrasonic anemometers", In: Proceedings of the *12th Symposium on Boundary Layers and Turbulence*, Vancouver, BC, Canada.

Whicker, J.J., Rodgers, J.C., Fairchild, C.I., Scripsick, R.C. and Lopez, R.C. (1997) "Evaluation of continuous air monitor placement in a plutonium facility", *Health Physics*, **2**, 734–743.

Yost, M.G. and Spear, R.C. (1992) "Measuring indoor airflow patterns by using a sonic vector anemometer", *American Industrial Hygienist Association Journal*, **53**, 677–680.